JOURNAL OF MATERIALS SCIENCE 19 (1984) 929–938

The setting of dental plasters: an electron microscopical study

K. R. WILLIAMS, G. J. WILLIAMS
Welsh National School of Medicine, Dental School, Cardiff, UK

A scanning electron and transmission microscopical study of commercial gypsum dental material has indicated an increased concentration of potassium at the material surface. The increased potassium concentration modifies the initial growth and subsequent morphology of the calcium sulphate dihydrate surface crystals. Calcium sulphate dihydrate nucleates at potassium sulphate "germ" nuclei leading to a higher density of small crystals. At higher local potassium concentration a new crystal phase (syngenite) forms, giving a thin surface layer about 15 μm deep. The formation of this new phase may modify the surface properties of model and die materials.

1. Introduction

The kinetics of the processes involved in the setting of gypsum [$CaSO_4 \cdot 2H_2O$; calcium sulphate dihydrate (CSD)] from pastes of calcium sulphate hemihydrate [$CaSO_4 \cdot \frac{1}{2}H_2O$; (CSH)] to form a strong hard cast has been investigated extensively by Ridge [1], Schiller [2] and Combes *et al.* [3]. The reaction is basically a simple one, involving the dissolution of CSH to form a supersaturated solution of Ca^{2+} and SO_4^{2-} ions, followed by the nucleation and growth of the new CSD phase, that is

$$CaSO_4 \cdot \tfrac{1}{2}H_2O + \tfrac{3}{2}H_2O \rightarrow CaSO_4 \cdot 2H_2O. \quad (1)$$

The reaction proceeds to the right because of the difference in solubility of the hemidydrate and dihydrate phases.

The reaction has generally been followed by indirect means, such as measurement of the reaction exotherm with time [1–3]. It is now recognized that the reaction involves classical nucleation and growth kinetics, giving rise to sigmoidal-shaped transformation curves (Fig. 1).

Accelerators and retarders are normally added to commercial stones and plasters in order to achieve the best consistency and setting times for the purpose in hand. Certain accelerators (in particular ionic salts such as K_2SO_4, KCl) influence the curve by both reducing the incubation time and increasing the overall rate of reaction (see Fig. 1), while others act as seeding nuclei with marked reductions in the incubation time but with little influence on the reaction rate. Calcium sulphate dihydrate typically acts in this latter way. The addition of accelerators and retarders also profoundly influences the morphology of growth of the CSD [4]. Because set plasters and stones are rather porous materials, a change in crystal morphology would be expected to influence markedly strength and hardness. Manufacturers typically add both accelerators and retarders to their stones and plasters in order to provide a consistent setting time. However, variations in the quantities of these additives will undoubtedly affect the mechanical properties through their influence on crystal morphology.

The present work was undertaken in order to examine directly the influence of, in particular, potassium sulphate on the size, type and number of CSD crystals forming during the setting process. The crystal morphology will then be related to the strength, hardness and consistency of the cast in a subsequent paper.

2. Methods and materials

Two CSH materials were examined, namely: (i) a commercial stone, Velmix; (ii) Analar calcium sulphate hemihydrate plaster to which varying concentrations of potassium sulphate were added. In

0022–2461/84 $03.00 + .12

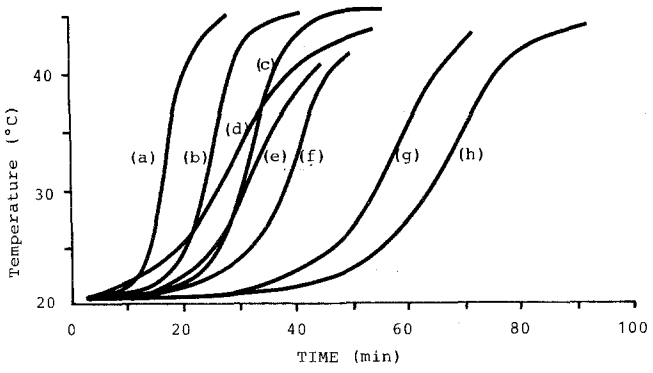

Figure 1 Curves of temperature plotted against time for mixtures of 60 g of water and 100 g of plaster accelerated in various ways: (a) sodium sulphate (1 g) added; (b) sodium chloride (1 g) added; (c) ammonium thiocyanate (1 g) added; (d) killed plaster (0.5 g) added; (e) mixture of water and plaster stirred vigorously for 6 min; (f) dry plaster ground for 30 min before mixing with water; (g) plaster ground for 15 min before mixing with water; (h) no additive (after Ridge [1]).

all cases, dilute suspensions were made up at a ratio of one part powder to ten parts water. The suspensions were either filtered, centrifuged or allowed several minutes standing, followed by extraction of the supernatant liquid onto glass slides (for optical and scanning electron microscopy) or carbon support films for scanning electron microscopy (SEM), or scanning transmission electron microscopy (STEM). Both the electron microscopes were equipped with an energy dispersive X-ray analysis (EDAX) facility.

3. Results

3.1. Optical examination

This work involved an examination of the number and type of crystals formed on addition of potassium sulphate accelerator. This procedure, although providing valuable information on the morphology and rate of growth of CSD, was unsatisfactory quantitatively because of local fluctuations in the concentration of Ca^{2+} and SO_4^{2-} ions on the glass slide.

Different CSD nuclei densities were observed on moving from the slide edge to the centre (Fig. 2). The potassium sulphate crystals were seen to nucleate first at the glass/air interface (Fig. 2).

3.2. SEM examination

3.2.1. Velmix stone

Several casts were made up in the conventional manner by mixing water and powder at 0.24 ratios. These pastes were then set against various surfaces. Fractured sections indicated the surface crystals to have a high concentration of potassium as well as showing a different crystal morphology from the cast interior (see Fig. 3). The surface crystals are generally smaller than in the interior.

3.2.2. Analar plaster

CSD crystals grown on glass slides from Analar CSH powder with K_2SO_4 additive were also examined in the SEM. Fig. 4 shows the needle morphology of the dihydrate crystals. Several needle-like cluster crystals have a high concen-

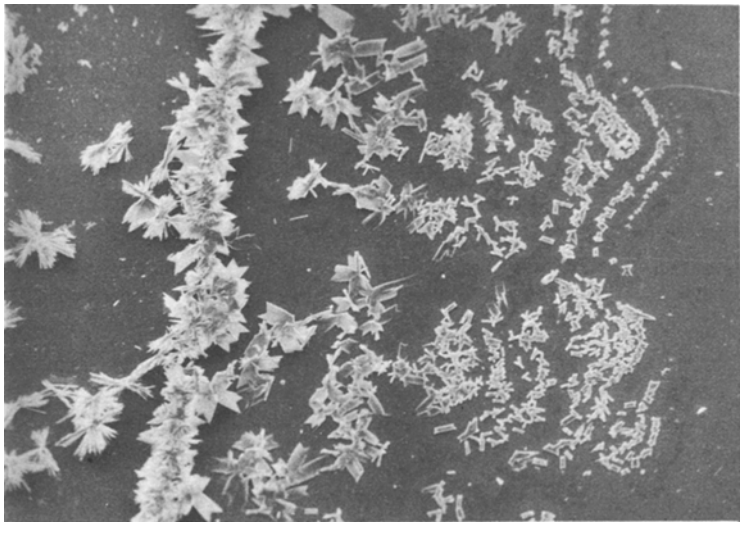

Figure 2 Optical micrograph of the distribution of calcium sulphate dihydrate density on formation on a glass slide.

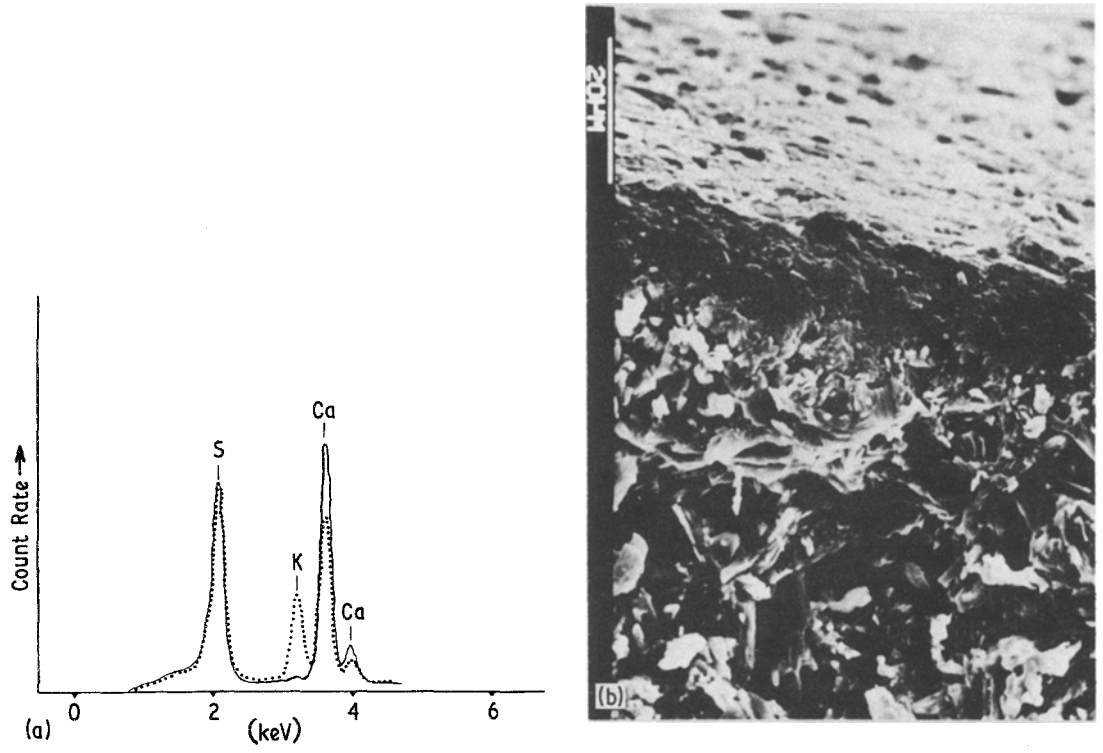

Figure 3 Composite figure showing the size and distribution of CSD at the surface after casting against glass and the concentration of potassium at the surface. · · · Analysis of surface; —— analysis of section. The accelerating voltage is 30 keV and the take-off angle 45°.

tration of potassium at their centres (Fig. 5), while other simple needle crystals growing in the same area contain no potassium. It should be noted that the potassium concentration in the crystals shown in Fig. 4 exists only over the diameter of the electron beam (≃ 10 nm). At higher concentrations of K_2SO_4 additive, potassium is generally incorporated into the dihydrate crystal, although the highest concentration remains at the crystal centre as shown on the composite micrograph, Fig. 6, obtained using potassium $K\alpha$ X-ray emission.

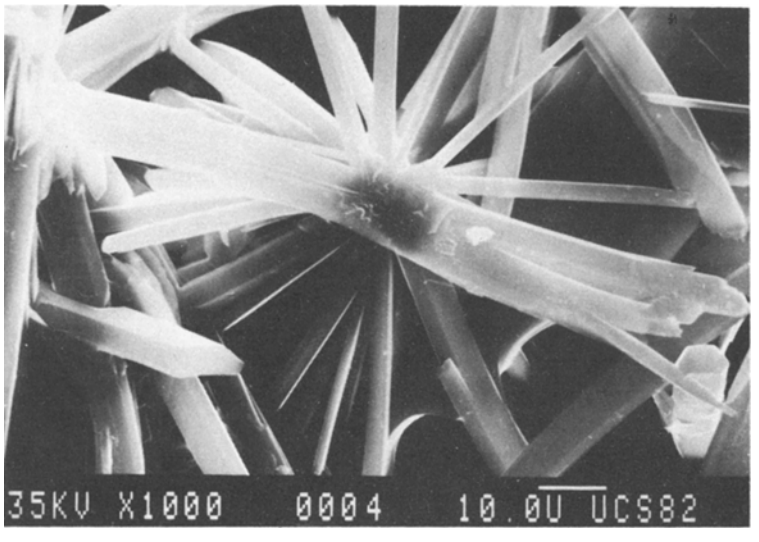

Figure 4 Calcium sulphate dihydrate crystal morphology an addition of potassium sulphate, i.e. preponderence of needle-like crystals.

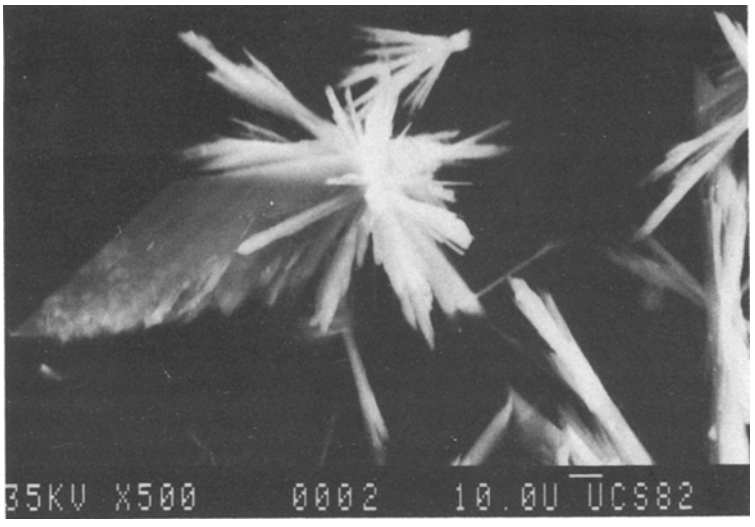

Figure 5 Scanning electron micrograph of CSD grown on glass slides with the potassium concentrated at the crystal centre.

3.3. STEM examination of plaster and stone

The STEM analysis of the as-received and set materials gave specific information about crystallographic and chemical composition of individual crystals. This procedure enabled the direct observation of the dissolution and setting reaction and the type of crystals formed.

Initially, a STEM analysis was carried out on crystals extracted from the surface of a standard set stone as shown in Fig. 3. The crystal morphology, EDAX analysis and diffraction pattern are shown in Figs. 7a to c. The diffraction pattern and chemical information are consistent with the syngenite phase $K_2SO_4 \cdot CaSO_4 \cdot 2H_2O$.

The as-received CSH crystals were collected on carbon support grids from an acetone–powder suspension, while the setting reaction was followed by allowing the crystals to grow directly on carbon support film.

Figs. 8 and 9 show the size and morphology of the as-received stone and plaster crystals. The stone material contains additions of both rutile (TiO_2) as a colouring agent and CSD and K_2SO_4 as accelerators. Quantitative EDAX analysis from a set polished section of Velmix stone indicates a potassium concentration of 0.3%. The dihydrate crystals, found in the as-received stone, are shown in Fig. 10. They are clearly faulted and remain stable under the electron beam.

The as-received Analar plaster CSH are similar in form to the stone material but contain a small proportion of filamentary CSD crystals growing from the hemihydrate surface. Dihydrate crystals grow from dilute suspension of this material, form-

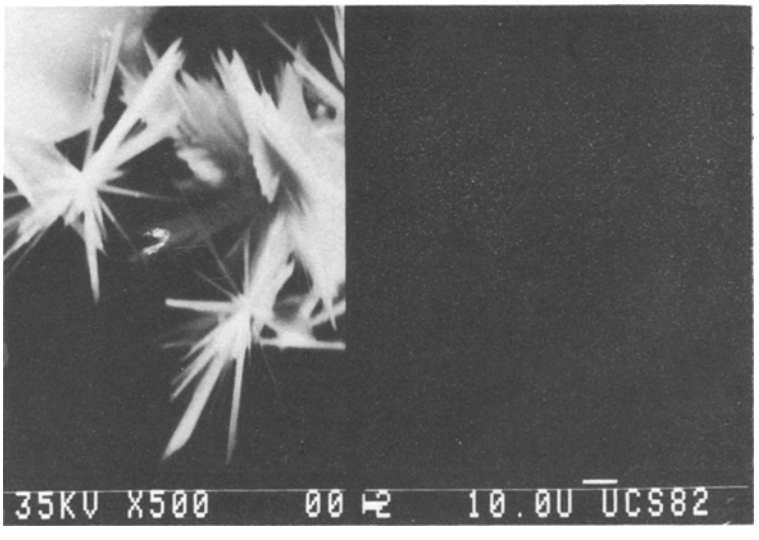

Figure 6 Composite micrograph showing the potassium distribution within the crystals at higher potassium sulphate additions.

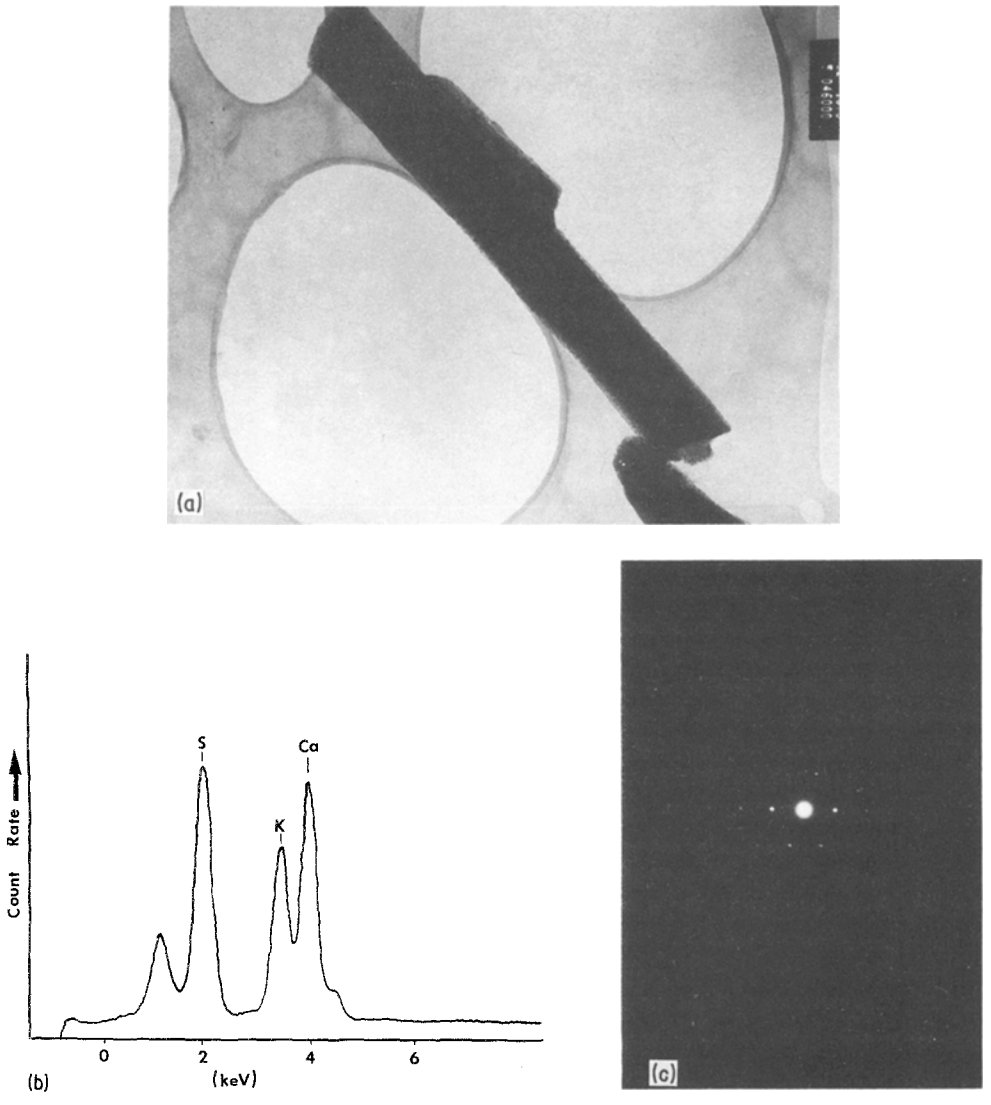

Figure 7 A scanning transmission electron microscopic analysis of surface crystals. (a) Micrograph of the crystals; (b) Selected area diffraction pattern; (c) X-ray analysis.

ing a dense mass between unreacted hemihydrate crystals (see Fig. 11).

Potassium sulphate additions significantly alter the CSD crystal morphology, as shown in Fig. 4. The dihydrate crystals exhibit predominately needle-like growth, with the needles appearing shorter and larger in diameter than in the absence of K_2SO_4. There is no evidence of unreacted hemihydrate crystals on slides where a K_2SO_4 addition has been made.

4. Discussion

The action of accelerators and retarders on the setting of plaster is little understood. It has been suggested that ionic salts speed up the rate of dissolution of the α-hemihydrate, resulting in higher local concentrations of Ca^{2+} and SO_4^{2-} ions at the growing dihydrate crystal surface and hence faster growth rates. Alternatively, more efficient nuclei may be formed by the addition of accelerators resulting in shorter induction periods and faster setting times. The second effect appears to be the operating mechanism when CSD is deliberately added in small quantities to commercial stones and plasters.

It is now generally recognized that the setting process is a classical nucleation and growth phenomenon giving rise to sigmoidal-shaped curves of transformation against time. Much of the understanding of these complex kinetics has come from

Figure 8 As-received stone.

the earlier work of Tammaun [5], Goler and Sachs [6], Mehl [7] and Avrami [8].

The Avrami theory was initially applied by Combes *et al.* [3] to the kinetics of hydration of autoclaved CSH, but discarded in favour of a modified theory [3], to take into account a point of inflection on the transformation curve. However, the Avrami [8] theories are particularly useful because they include important assumptions based on experimental facts. These include:

1. The new phase is nucleated by "germ nuclei" already existing in the old phase;
2. The number of germ nuclei per unit region at time t, decrease in two ways
   (a) through becoming active growth nuclei;
   (b) through being consumed by grains of the new phase, whose linear dimensions are growing at rate G.
3. The ratio of the growth rate G to the probability of a germ nucleus becoming a growth nucleus, n, is approximately independent of temperature and concentration in a given "isokinetic range", i.e. G/n.

For a given substance and crystal habit Avrami showed that

$$V_{\text{lex}} = \sigma\alpha^3 \int_0^{\tau} (\tau - z)^3 N(z)\, \mathrm{d}z$$

for pseudospherical or polyhedral grains, where α is a shape factor, $n\,\mathrm{d}t = \mathrm{d}\tau$, z is the time and V_{lex} the extended crystal volume.

Two other important situations were con-

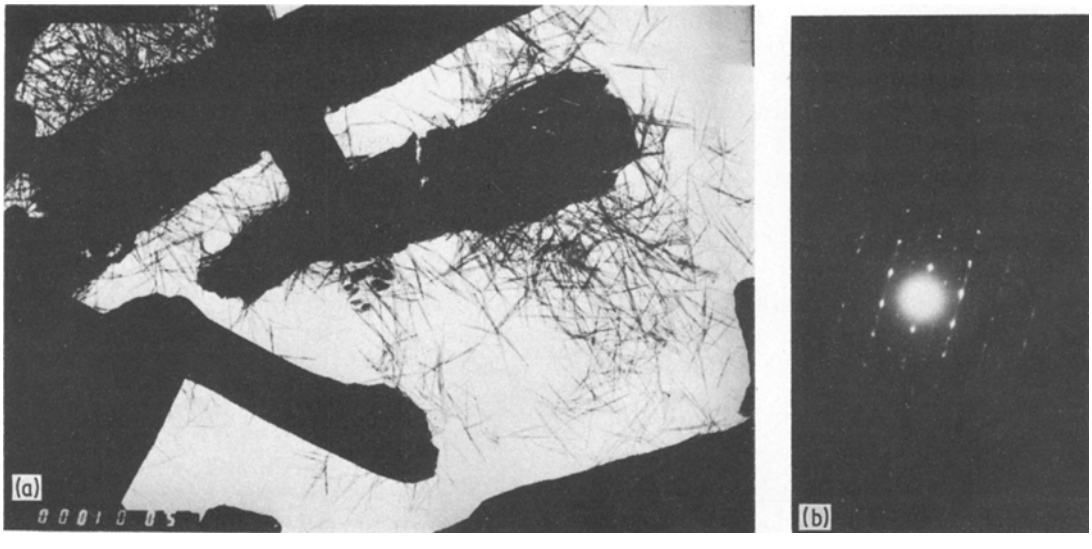

Figure 9 As-received plaster. (a) micrograph crystals; (b) selected area diffraction pattern.

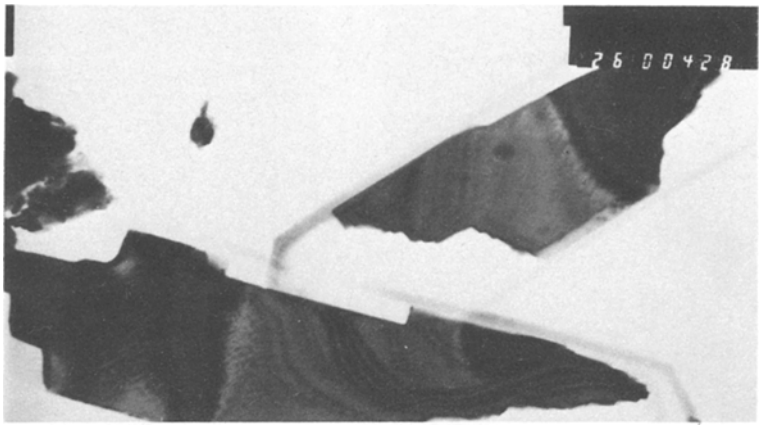

Figure 10 Faulted dihydrate crystal in the as-received stone.

sidered, where (a) the growth is primarily along two dimensions so that the grain is plate-like in shape, and (b) where growth is primarily along one direction resulting in needle-shaped grains. The growth expressions corresponding to these two growth modes are

$$V_{\text{lex}} = \sigma\alpha^2 \int_0^\tau (\tau - z)^2 N(z)\, dz$$

and

$$V_{\text{lex}} = \sigma\alpha \int_0^\tau (\tau - z) N(z)\, dz.$$

The transformed matter $(1 - V)$ is related to the ratio of the non-overlapped volume V^1 to the extended volume V_{lex}, i.e.

$$\frac{V^1}{V_{\text{lex}}} = 1 - V$$

or

$$\frac{V^1}{1 - V} = \bar{N} \int_0^\tau e^{-z} \nu(\tau, z)\, dz$$

resulting in the following set of equations for crystal growth (where $\nu(\tau, z)$ is the volume of a grain at time τ which began growth from a nucleus at time z):

Polyhedral: $V = 1 - \exp[(-\sigma G^3 N n t^4)/4]$

Plate-like, n small:

$$V = 1 - \exp[(-\sigma' G^2 \bar{N} n t^3)/3]$$

Plate-like, n large: $V = 1 - \exp(-\sigma' G^2 \bar{N} t^2)$

Needle-like, n small:

$$V = 1 - \exp[(-\sigma'' G \bar{N} n t^2)/2]$$

Needle-like, n large: $V = 1 - \exp(-\sigma'' G \bar{N} t)$.

These equations may be written generally as $V = 1 - \exp(-Bt^k)$.

The shape and position of the curves on the isothermal transformation plot will indicate the type of reaction product formed. Thus the

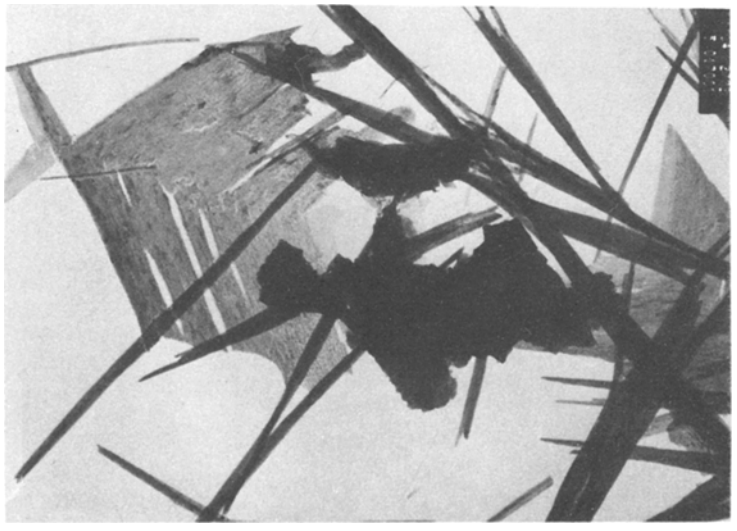

Figure 11 Dihydrate crystals growing between unreacted α-hemihydrate.

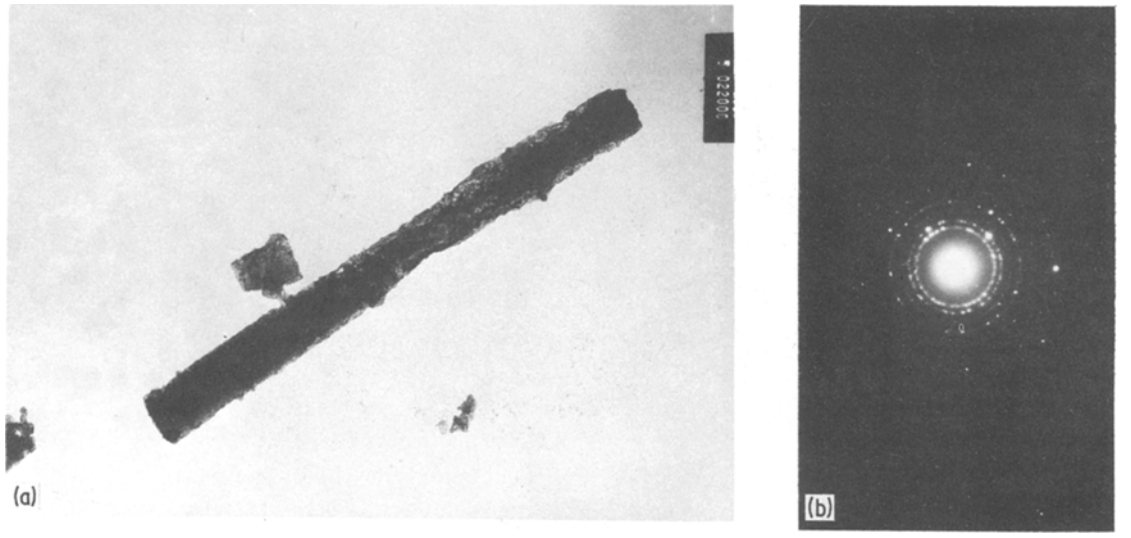

Figure 12 (a) Dehydrated CSD crystal. (b) Selected area diffraction pattern.

reaction curves become increasingly flat as the growth changes from polyhedral to a needle-like shape. The forms of the predicted reaction curves are shown in Fig. 13 and may be compared with actual reaction curves (Fig. 1) from Ridge's original work. Avrami [8] suggested a simple means of comparing with experiment, the difference in crystal shape between the various limiting cases by taking the ratio of times for two fixed degrees of transformation. For convenience the ratios at 75% and 25% transformation were taken as an index. Since $\log(1-0.75)/\log(1-0.25) = 4.82$, the various limiting cases will have fourth, third, second and first roots of this ratio. Thus:

$$1.48 \leqslant \frac{t_{0.75}}{t_{0.25}} \leqslant 1.69 \text{ for polyhedral growth}$$

$$1.69 \leqslant \frac{t_{0.75}}{t_{0.25}} \leqslant 2.2 \text{ for plate-like growth}$$

$$2.2 \leqslant \frac{t_{0.75}}{t_{0.25}} \leqslant 4.82 \text{ for needle-like growth.}$$

The work of Avrami [8], therefore, provides a basis for the examination of accelerators on crystal morphology and hence the mechanical properties and surface hardness of the set plasters and stone. In a related study [9], it has been found that a set commercial stone has a high incidence of potassium at the cast surface compared with the interior (see Fig. 3). A quantitative analysis of the potassium concentration at the case interior indicated a value of 0.3%, while this value is increased by approximately ten times at the case surface. This concentration effect is quite general and appears when the pastes are cast against several surfaces. This effect is however absent when very small quantities are cast in thin sections. Presumably the concentration effect is a consequence of the setting exotherm resulting in concentration of potassium at the cooler surface (Fig. 2). Concentration of potassium at the surface influences the morphology of the set CSD crystals, as seen in Fig. 3. In all cases the CSD grain size when examined in the SEM is smaller at the surface than in the grain interior. The higher incidence of CSD crystals in the presence of potassium may arise from the presence of more growth nuclei, either as a result of the growth of CSD on potassium sulphate germ nuclei, or because potassium sulphate influences the rate of dissolution of the CSH thus increasing the Ca^{2+} and SO_4^{2-} ion concentration in solution

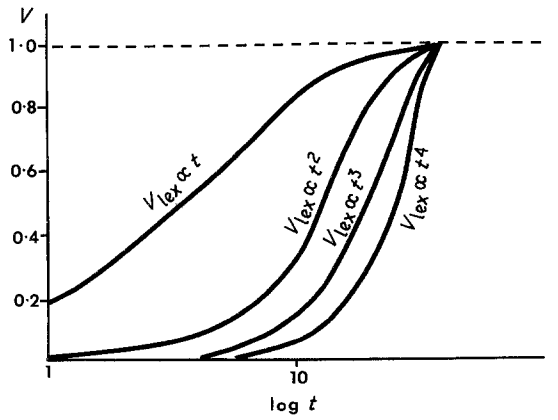

Figure 13 Transformation–time curves for polyhedral, plate-like and needle-like growth of crystals (after Avrami [8]).

and hence the rate of homogeneous nucleation. The latter explanation is unlikely, since the growth nuclei arise from an original population of "germ nuclei", i.e. the nucleation of CSD is heterogeneous. Examination of gypsum crystals grown from supernatant liquid do not generally indicate increased numbers of nuclei until the potassium sulphate concentration approaches 10%. At this potassium sulphate concentration the needle-like morphology is generally dominant with the needles generally thicker and less angular than in the absence of or at lower concentrations of potassium sulphate (Fig. 4). Gypsum crystals grown in the presence of potassium sulphate additions indicate a potassium concentration at the crystal centre (presumably the nucleation site). At lower levels of potassium the concentration is discrete, existing only over the diameter of the electron beam, 10 nm (Fig. 5). This effect persists at higher potassium sulphate concentration but in addition the potassium is also included in the crystal arms, as shown on the composite photograph of Fig. 6.

Crystals removed from the surface of a commercial cast, typically that of Fig. 3, are shown in Fig. 7. Crystal diffraction analysis together with EDAX indicate a $K_2SO_4 \cdot CaSO_4 \cdot 2H_2O$ syngenite phase. The effect of this layer on surface profiles will be discussed in an associated paper.

Clearly, potassium sulphate is associated with CSD nucleation and growth. It is difficult to ascertain quantitatively from the present experiments the incidence of nuclei density. Examination of crystal nucleation and growth from dilute filtered or centrifuged suspensions has been criticized by Ridge [1] due to the removal of natural impurity particles which may be adding to the numbers of "germ nuclei". However, it is clear from the present work that potassium influences the shape and numbers of CSD crystals grown from dilute suspensions. Evidently the addition of ionic salts reduces the incubation period of growth (Fig. 1). In the case of potassium sulphate additions, this effect would appear to be the result of an increased probability of the formation of growth nuclei from potassium sulphate germ nuclei rather than on random fluctuations of Ca^{2+} and SO_4^{2-} ion concentrations, enabling homogeneous nucleation or heterogeneous nucleation on undefined particles. The morphology of growth is also affected by potassium additions, as shown in Fig. 6. This behaviour is expected if, as has been assumed by previous workers, the rate of dissolution of CSH is increased by ionic salt additions. Under these circumstances the higher Ca^{2+} and SO_4^{2-} ion concentration will result in a higher driving force for growth with the result that at the higher rates of transformation the crystal morphology should change to a more efficient growth mode, such as needle-like growth, if previously a plate-like or polyhedral morphology existed. This behaviour is in fact observed on addition of potassium sulphate to plaster suspensions (Fig. 4).

Potassium sulphate additions also appear to influence the efficiency of dissolution of the CSH phase. The majority of slides examined of CSD crystals grown from dilute suspensions of pure $CaSO_4 \cdot \frac{1}{2}H_2O$ showed a substantial number of partly reacted or unreacted original CSH crystals within the set CSD matrix (see Fig. 11). The addition of even small quantities of potassium sulphate (1% concentration) to the pastes resulted in the complete elimination of the CSH phase, suggesting a more efficient dissolution process.

4.1. Crystal morphology

In view of the importance of crystal size and morphology on properties, it is instructive to comment at this stage on some of the observations made in this work.

The fishtail or plate-like crystals grow at the intersection of the needle-like CSD crystals (Fig. 9). Both types of CSD crystals grow at the surface of freshly prepared (2 days) Analar $CaSO_4 \cdot \frac{1}{2}H_2O$. The fish fail crystals are thin lamellae, as shown on the micrograph, and substantiated by the streaked and fragmented diffraction pattern. The lamellar crystals grow incrementally by gathering tiny needle crystallites already existing in suspension. These crystallites are presumably prevented from becoming "growth nuclei" because of the falling Ca^{2+} and SO_4^{2-} ion concentrations as the reaction proceeds. They are also particularly unstable and readily dehydrate under the heating effect of the electron beam to form anhydrous calcium sulphate. The lamallae fragment during dehydration to form tiny equiaxed crystallites and the discrete SAD spot pattern reverts to a polycrystalline ring pattern (Fig. 12).

The ratio of plate-like to needle-like crystal morphology should be strongly reflected in the shape of the transformation curve. This if needle-like morphology persists throughout the setting process, the reaction rates are fast and the trans-

formation against time curve relatively flat, implying a high incident of growth nuclei and high a driving force for growth. Such conditions can only exist at high and persistent levels of Ca^{2+} and SO_4^{2-} ion concentrations as when accelerators which influence the rate of dissolution of the CSH are present. In the absence of ionic accelerators, the needle-type morphology is concentrated on partly dissolved CSH (Fig. 11). The local Ca^{2+} and SO_4^{2-} concentrations are high at such sites, and diffusion distances small, with the result that potentially fast growth rates are possible. Under such circumstances the needle-like morphology results, as indicated from Avrami's work.

5. Conclusions

The addition of potassium sulphate to stone and plaster powder both influences the incidence of CSD nuclei and also the resulting growth rate of the CSD. Additionally the CSD crystal morphology influences the surface properties of the resulting cast.

Casts of commercial stone set against typical impression material surfaces indicates a high concentration of potassium to a depth of about 15 μm. The crystal morphology at the surface is consequently modified, resulting in a layer of small, predominantly needle-like crystals. At the outer extremity the crystals become the syngenite phase, $K_2SO_4 \cdot CaSO_4 \cdot 2H_2O$. Direct observation of many crystals indicated a high level of potassium at their centres, suggesting that the CSD phase was nucleated at K_2SO_4 crystals. At higher potassium levels, the potassium sulphate is generally distributed throughout the crystal with the formation of the syngenite phase. Clearly surface properties may be extremely sensitive to the level of potassium additive to the case dimensions.

References

1. M. J. RIDGE, *Rev. Pure Appl. Chem.* **10** (1960) 243.
2. K. K. SCHILLER, "Mechanical Props of Non-Metallic Brittle Materials", edited by W. H. Walton (Butterworths, London, 1958) pp. 35–49.
3. E. C. COMBE, D. C. SMITH and M. BRADEN, *J. Appl. Chem.* **20** (1970) 287.
4. J. K. HARCOURT and E. P. LAUTENSCHLAGER, *J. Dental Res.* 49 (1970). 502.
5. G. TAMMAUN, "Kristallisieren und Schmelzen" (Leipzig, 1903).
6. F. GOLER and G. SACHS, *Z. Phys.* 77 (1932) 281.
7. R. F. MEHL, "The Physics of Hardenability", Symposium on Hardenability (American Society for Metals, Detroit, 1938).
8. M. AVRAMI, *J. Chem. Phys.* 7 (1939) 1103.
9. G. J. WILLIAMS, M. Phil. Thesis, Polytechnic of Wales (1982).

Received 28 March
and accepted 21 July 1983